A computational investigation of the role of moisture in live fuels subject to pyrolysis and ignition through convective heat transfer

B. L. Yashwanth B. Shotorban S. Mahalingam*

+Department of Mechanical and Aerospace Engineering,
The University of Alabama in Huntsville, Huntsville, AL 35899, USA
*Corresponding Author Email: babak.shotorban@uah.edu

In this work, the role and distribution of moisture during thermal degradation and gas phase combustion of a horizontally oriented solid fuel element representing living vegetation subjected to convective heating is investigated numerically. The dimensions of a typical manzanita leaf (*Arctostaphylos glandulosa*) were used to represent the solid fuel. An improved three dimensional computational model that simultaneously resolves both solid phase thermal degradation and gas phase combustion (Lautenberger, 2014) has been used. The model uses Gpyro3D for solid phase degradation and FDS for gas phase combustion. A 12-step kinetic reaction scheme (Miller & Bellan, 1997) that accounts for evaporation of moisture, and pyrolysis of solid fuel has been incorporated. The reaction scheme was validated with experimental TGA results of Koufopanos *et al.* (1989) and numerical results of Miller & Bellan (1997). Ignition of the solid fuel at three initial moisture contents (40, 76, 120%) exposed to a convective source was simulated. For similar moisture content, the ignition time and burnout time compared closely with the experimental results of Pickett *et al.* (2010). Lower moisture content resulted in earlier onset of pyrolysis and ignition resulting in higher solid and gas phase temperatures. Local moisture evaporation and temperature rise were observed initially at the periphery of the solid fuel in all the three cases. The numerical results suggested that moisture content influenced the process of pyrolysis and ignition of live fuels.

Keywords: Live fuels, Wildland fires, Pyrolysis, CFD, Convection

1 Introduction

Wildland fires can threaten life, property, and natural resources, or they can perform necessary ecological functions throughout the world. A large number of fires occur in live fuels that contain significant moisture [1]. Fires that burn through large areas of live vegetation often consists of smaller fuel elements such as leaves, twigs and branches. The ability to predict the spread of these wildland fires in live fuels is paramount in protecting both property and ecology.

When a solid fuel/biomass particle is heated to a sufficiently high temperature, it undergoes thermal degradation. Thermal degradation occurs in two sequential steps. The first step is pyrolysis, which is usually an endothermic process that breaks down the forest matter into low molecular mass gases (volatiles), tars, carbonaceous char and mineral ash. The second process is burning, which is an exothermic process known as combustion. Ignition is a transition process between the first and second step. Hemicellulose, cellulose and lignin are the three main components of

biomass and they in general cover respectively 20–40, 40–60, and 10–25 %wt. [2]. It was also suggested by [3] and [4] that the pyrolysis of any biomass can be considered as the superposition of these three main components . Thus the knowledge of pyrolysis characteristics of cellulose, hemicellulose and lignin is the basis for a better understanding of biomass thermo-chemical conversion.

Chemical reactions of biomass materials exposed to high temperature sources can be roughly classified as primary and secondary reactions. Primary reactions are concerned with the degradation of the solid fuel into char and numerous volatile products whereas secondary reactions are those undergone by primary volatile products [5]. The first kinetic models were proposed in the 1960s by Kilzer and Broido [6], Chatterjee and Conrad [7] and Shafizadeh [8], and are the basis of more recent kinetic models. Several investigators have developed multi-step kinetic models more or less derived from the original mechanism of Kilzer and Broido [6]. Bradbury *et al.* [9] reformulated Broido's reaction model by introducing active cellulose, as an intermediate species between native cellulose and reaction products and this reaction model is called as 'Briodo–Shafizadeh model (BS)'. Di Blasi [5] in her numerical work used the BS model of cellulose pyrolysis and extended it to include secondary reactions concerning the tar cracking which is known as extended Briodo–Shafizadeh model. Miller & Bellan used the extended BS model as a "skeleton" and formulated a superposed kinetic scheme for cellulose, hemicellulose and lignin kinetics. This model has been incorporated in the present work as a reaction mechanism for the three primary biomass components involving multi-step kinetics for competitive primary pyrolysis and secondary tar decomposition reactions.

Fuel moisture content (FMC) present in the plant matter is an important factor that influences the burning behaviour of live fuels [10]. Water affects ignition processes involving both solid and gas phases. According to [11], if all of the water within the fuel does not evaporate prior to ignition, then the water vapor will dilute the gaseous pyrolyzates, making it more difficult to generate a flammable mixture. According to Pickett *et al.* [12], who investigated the burning of various live leaf samples in detail using the Flat Flame Burner (FFB) apparatus, ignition does not occur at the end of global evaporation, as predicted by conventional models, but possibly at the end of local evaporation. They also found that a significant amount of moisture (30–60%) remains in the sample for most species at the time of ignition. However, their experiments did not focus on pyrolysis and other physical processes inside the fuel while it pyrolyses. Experiments conducted by McAllister *et al.* [1] also reveal that there exists considerable amount of temperature and moisture gradients inside the solid during pyrolysis of moist fuels which are assumed to be thermally thin.

The main aim of the present work is to better understand the effects of moisture content on pyrolysis and gas phase ignition of a solid fuel composed of cellulose, hemicellulose and lignin by accounting the multi-step thermo-physical processes using a three-dimensional solid-gas model. The solid model uses Gpyro3D [13] for pyrolysis and the gas phase fluid dynamics and ignition is solved using Fire dynamic simulator (FDS) [14]. In the present study, ignition time is defined as the time at which the heat release rate (HRR) becomes positive in the gas phase over the surface of cellulose element. Any value above this would mean an active flame in the simulation.

2   Physical configuration

In a spreading wildland fire, unburnt vegetation that lies ahead of burning vegetation is exposed to varying combinations of convective and radiative heating. The focus of the present work is on an analysis of the effect of FMC during ignition achieved via convection heating of a thin, rectangular biomass material representing a live fuel. The fuel element we choose is three-dimensional ($0.03 \times 0.03 \times 0.002$ m, L$\times$W$\times$T) with fixed thickness. The choice of this configuration is motivated by its similarity to experimental configurations studied by Pickett *et al.* [12]. A schematic of the physical domain along with the boundary conditions is shown in fig. 1(a). The computational domain used for the gas-phase solver FDS, is a rectangular cube of size $x = 0.18$ m, $y = 0.18$ m and $z = 0.32$ m. The grid resolution used in x, y and z directions is $120 \times 120 \times 160$, respectively. The solid fuel particle is centered in the gas-phase domain and located at $z = 0.05$ m. The initial temperature, moisture content, pressure, gaseous species mass fractions, and condensed phase species were set uniform throughout the solid. Fuel element is simulated as a separate region modeled by Gpyro3D with a grid spacing of 0.0006 m in the x and y directions and 0.0003 m along the depth. Here, 9600 grid cells are used for Gpyro3D. The fuel element is exposed primarily to convective heating due to the modeled burner having dimensions of 0.075×0.03 m, L $\times$ W. Heated air at a temperature of 1100^oC enters the domain through this burner at $t = 0$s.

All the computations were performed using message passing interface (MPI) protocol using 36 processors of Dense Memory Cluster (DMC) located at Alabama Supercomputer Authority. A typical simulation of 20 seconds required a wall time of 72 hours and 64 GB of memory.

3   Reaction mechanism and computational models

A considerable amount of temperature and moisture variation was observed along the surface of fuel by Pickett *et al.* [12] and according to McAllister *et al.* [1] these gradients were observed along the depth of the fuel, indicating a three-dimensional nature of pyrolysis. To investigate the three-dimensional effects during fire initiation and propagation on fuel elements where multidimensional heat and mass transfer effects are significant, a fully coupled Gpyro3D-FDS model is used. Detailed descriptions of mathematical models with main assumptions and governing equations used in Gpyro3D and FDS are given in [13] and [14], respectively. Initially, the condensed/solid phase domain consists of moisture, cellulose, hemicellulose, lignin and the gas phase within the solid fuel consists of air (nitrogen and oxygen). Their respective initial mass fractions are given in Table 1. The initial mass fractions of other species were considered negligible. The initial temperature was set to be the ambient temperature of 300K.

The skeleton of the cellulose scheme outlined by Di Blasi [5] is shown in fig. 1(b). Reactions R1, R2, R3 are primary reactions and R4 is a secondary reaction. The primary reactions are concerned with the conversion of the virgin species to active state which later breaks down to lower molecular weight gases while the secondary reaction, which is an oxidation reaction, is concerned with the tar breakdown to low molecular weight gases. The term "virgin" refers to reactants cellulose, hemicellulose and lignin which follow the same reaction pathway (R1–R4). In the current study, reaction R5 represents two evaporation reactions and has been incorporated to account for moisture evolution based on free and bound state. Free moisture evaporation reaction has been adopted from [15] and bound state evaporation has been adopted from [16]. This 12-

step reaction model has been incorporated in Gpyro3D. The reaction kinetics and thermo-physical properties for reactions R1-R5 are opted from [15], [16] and [17]. The thermophysical properties were assumed to be identical for cellulose, hemicellulose and lignin. Thermal conductivity and specific heat capacity were considered as temperature dependent following correlations used for soft wood species in [18]. The properties for the gas species present within the solid fuel were assumed from the available data for air.

4 Results and Discussions

Initially, the 12-step reaction mechanism has been validated against the experimental data of Koufapounas *et al.* [19] and numerical results of Miller & Bellan [17]. Koufapounas *et al.* [19], heated beech wood to generate experimental themogravimetric analysis (TGA) data at a heating rate of 5 and 20 K/min. Miller & Bellan [17] validated their numerical data against the experimental TGA data at similar heating rates. In the current study, a zero-dimensional model of Gypro was used to predict both experimental data of Koufapounas *et al.* [19] and numerical results of Miller & Bellan [17]. The reaction R5 was neglected during this validation, since the experiments and numerical study did not consider a moist specimen. As seen in fig. 2, the residual mass predicted for this setup is in good agreement with its experimental and numerical counterpart.

In order to model the ignition of individual manzanita leaf species used during the experimentation of Pickett *et al.* [12], the 12-step reaction mechanism has been incorporated into Gpyro3D along with the coupled FDS model with similar boundary conditions (fig. 1(a)). The time history of mass loss rate (MLR) obtained for a case of FMC 76% during the simulation has been compared with its experimental counterpart and is shown in fig. 3(a). The time at which MLR values became positive can be treated as the initiation of evaporation, mainly due to formation of water vapor. In case of simulations, this occurred at $t = 2$s and in experiments it occurred at $t = 1$s. Also, its is observed in this figure that the simulation over predicts the experimental data. This overpredicion was believed to be due to the difference in initial mass of the solid fuel considered in the simulations and experiments. The initial mass in the numerical simulations was 1g, whereas in the experiments it was 0.3g for the data presented here. The time history of normalised mass between the simulation and experimental results is shown in fig. 3(b). The burn out time in the simulation was close to $t = 13$ s, whereas in experiments it was close to $t = 15$s.

The time histories of overall MLR and HRR are plotted in fig. 4 (a,b) for a FMC of 40, 76 and 120%. In fig. 4(a), water vapor released by evaporation of free and bound water, and fuel vapor, which pyrolyzates from cellulose, hemicellulose and lignin were the species that diffused from the solid phase to the gas phase domain surrounding the solid fuel. The initiation of evaporation reaction occurred at $t = 2$s for a FMC of 40, 76 and 120%. It is noted that the MLR curves for each of these FMC cases exhibited two overall peaks. The first peak is caused by evaporation of the free water and the second peak is caused by the combined contribution of fuel vapor and water vapor from fuel and bound water evaporation, respectively. Oxidation of the gaseous fuel vapors resulted in flaming combustion. In fig. 4(b), HRR quantifies the amount of heat generated due to stoichiometric combustion of fuel vapors with oxygen in the gas phase. The fuel vapors were modeled as methane and are assumed to react at stoichiometric proportion with air. The ignition time for 76% FMC case in the simulation was $t = 7.5$s and in the experimental counterpart it was

close to 8s. Also from this figure, it is clear that FMC affected the time at which ignition occurred as the ignition times were $t =6$, and 8s for FMC of 40, and 120% respectively.

Two-dimensional contours of temperature and mass fraction of water vapor are plotted in the gas phase along an xz slice located at $y = 0$ for a FMC of 76% as shown in figs 5(a) and (b) at $t =3$s. Heated air exits the burner and it encounters the solid fuel along the path as shown in fig. 5(a). The solid fuel acts as an obstruction essentially causing flow separation. As a result of this, coherent structures are generated above the solid fuel which are convected out of the computational domain. Figure 5(b) shows water vapor generated around the solid fuel as a result of free moisture evaporation. Free moisture gets converted to water vapor before the initiation of gas phase ignition due to its low activation energy and is transported as a passive scalar. Two-dimensional contours of temperature and mass fraction of water vapor are plotted in the gas phase along an xz slice located at $y = 0$ for an FMC of 76% as shown in figs. 6(a) and (b) at $t =8$s. As discussed before the solid fuel at this instant has underwent ignition, therefore the temperatures in the vicinity of the solid fuel are high as illustrated in fig. 6(a). The periphery of the solid fuel ignites prior to the center as a result of a stagnation zone. The stagnation zone is formed below the center of the solid fuel resulting in low values of heat transfer coefficient in that region. Following this in fig. 6(b), high mass fraction of water vapor was observed close to the periphery compared to the center of the solid fuel. The water vapor here is formed due to the evaporation of bound moisture from the solid fuel. From this figure it is clear that bound moisture evaporation front follows the free moisture evaporation during the ignition process. These observations indicate that the evaporation and ignition processes occur together in live fuels and are consistent with the experimental findings of Pickett *et al.* [12].

5 Summary and Conclusions

The effect of moisture content on pyrolysis and ignition of a thin solid fuel particle subjected to heating by convection has been investigated numerically. The 12-step thermal degradation reaction mechanism used was initially validated with other TGA experiments and numerical simulation. Later using the three dimensional computational model, it was compared with the experimental data obtained using the FFB apparatus with convection as the heating source. The simulations were consistent with the experimental results in terms of ignition and burnout time prediction, fire initiation and spread pattern, however the MLR data was over predicted due to the high initial mass of the solid fuel. A FMC of 40, 76 and 120% was considered to study the effect of moisture content. The temperature response and thermal degradation rate was higher for the case with 40% FMC and ignition occurred prior to the 120% FMC case. Local evaporation of moisture and temperature rise at the periphery of the solid fuel was observed, also a significant amount of moisture remained in the sample at the time of ignition indicating that different points in the domain pyrolyze at different times. High mass fraction of water vapor was observed in the ignition zone clearly manifesting the point that evaporation and combustion can occur together in live fuels.

6 Acknowledgments

tive agreements 11-JV-11272167-103 with The University of Alabama in Huntsville. The authors thank Christopher W. Lautenberger for providing assistance on configuring and using Gpyro3D coupled with FDS.

References

[1] S. McAllister, I. Grenfell, A. Hadlow, W.M. Jolly, M. Finney, and J. Cohen. *Fire Saf. J.*, 51 (2012) 133 – 142.

[2] H. Yang, R. Yan, H. Chen, D. H. Lee, and C. Zheng. *Fuel*, 86 (2007) 1781 – 1788.

[3] J. J. Manya, V. Enrique, and L. Puigjaner. *Ind. Eng. Chem. Res.*, 42 (2003) 434–441.

[4] T. R. Rao and A. Sharma. *Energy*, 23 (1998) 973–978.

[5] C. D. Blasi. *Biomass Bioenergy*, 7(1-6) (1994) 87 – 98.

[6] F. J. Kilzer and A. Broido. *Pyrodynamics*, 2 (1965) 151 – 163.

[7] P.K. Chatterjee and C.M. Conrad. *Text. Res. J.*, 36 (1966) 487.

[8] F. Shafizadeh. Pyrolytic reactions and products of biomass. In R. P. Overend, T. A. Milne, and L. K. Mudge, editors, *Fundamentals of Thermo-Chemical Biomass Conversion*, pages 183 – 217. 1985.

[9] A. G. W. Bradbury, Y. Sakai, and F. Shafizadeh. *J. Appl. Polym. Sci.*, 23 (1979) 3271–3280.

[10] C. M. Countryman. *Fire Management Notes*, 35 (1974) 10–14.

[11] S. C. Ferguson, A. Dahale, B. Shotorban, S. Mahalingam, and D. R. Weise. *Combust. Sci. Technol.*, 185 (2013) 435 – 453.

[12] B. M. Pickett, C. Isackson, R. Wunder, T. H. Fletcher, B. W. Butler, and D. R. Weise. *Int. J. Wildland Fire*, 19 (2010) 153 – 162.

[13] C. W. Lautenberger. *Fire Saf. Sci. (IAFSS Symposium)*, (2014) .

[14] K. McGrattan, S. Hostikka, J. Floyd, H. Baum, and R. Rehm. Fire Dynamics Simulator, Version 5. Technical Reference Guide, NIST, 2007.

[15] K. M. Bryden, K. W. Ragland, and C. J. Rutland. *Biomass Bioenergy*, 22 (2002) 41 – 53.

[16] D. R. Prince and T. H. Fletcher. A combined experimental and theoretical study of the combustion of live vs. dead leaves. In *8th US National Combustion Meeting of the Combustion Institute, Park City, UT*, 2013.

[17] R. S. Miller and J. Bellan. *Combust. Sci. Technol.*, 126 (1997) 97 – 137.

[18] Z. T. Yu, X. Xu, L. W. Fan, Y. C. Hu, and K. F. Cen. *For. Product. J.*, 61 (2011) 130–135.

[19] C. A. Koufopanos, A. Lucchesi, and G. Maschio. *Can. J. Chem. Eng.*, 67 (1989) 75–84.

Table 1: Initial mass fractions

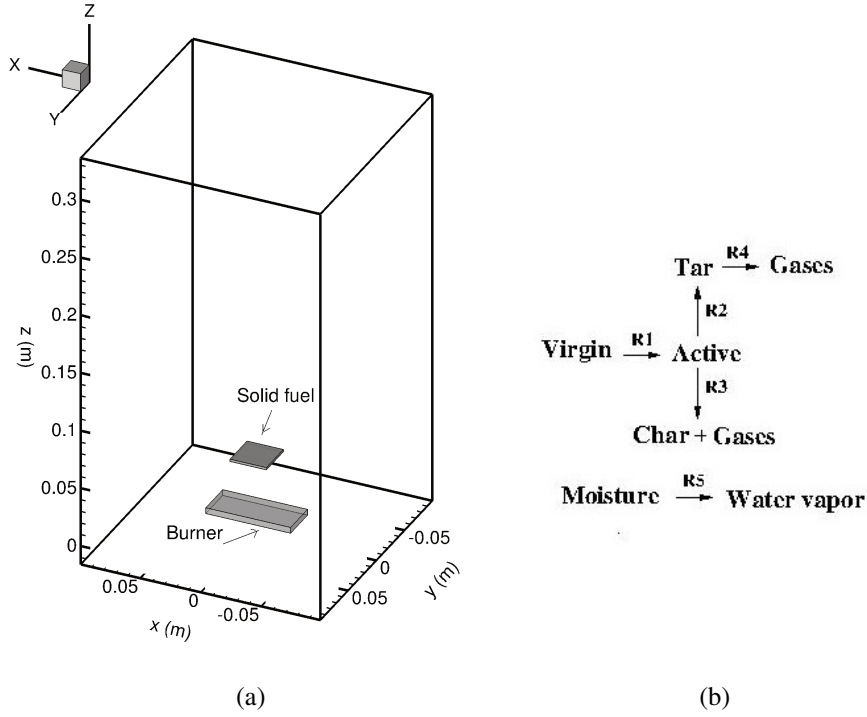| FMC	Free moisture	Bound moisture	Cellulose	Hemicellulose	Lignin	N_2	O_2
40%	0.2175	0.0725	0.2272	0.2272	0.2556	0.77	0.23
76%	0.315	0.105	0.19	0.19	0.20	0.77	0.23
120%	0.4125	0.1375	0.144	0.144	0.162	0.77	0.23

Figure 1: (a) Isometric view of computational domain showing thin solid fuel subjected to convective heating from the burner, (b) Generic reaction scheme used to model cellulose, hemicellose and lignin pyrolysis (Miller & Bellan [17]) along with vaporization reaction of moisture.
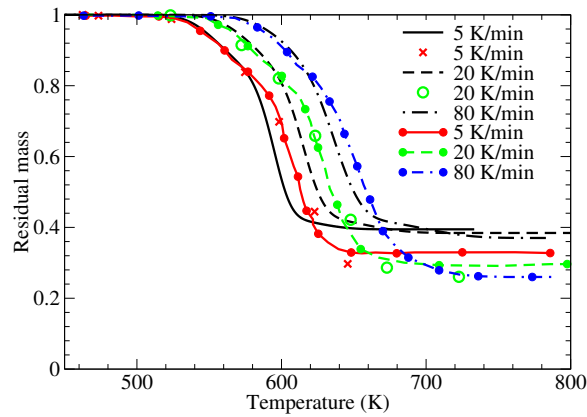

Figure 2: Results obtained in the current study (dark line) with simulation results of Miller & Bellan [17] (colored line with symbols) and TGA experimental results of Koufopanos *et al.* [19] (colored symbols) for various heating rates.

7
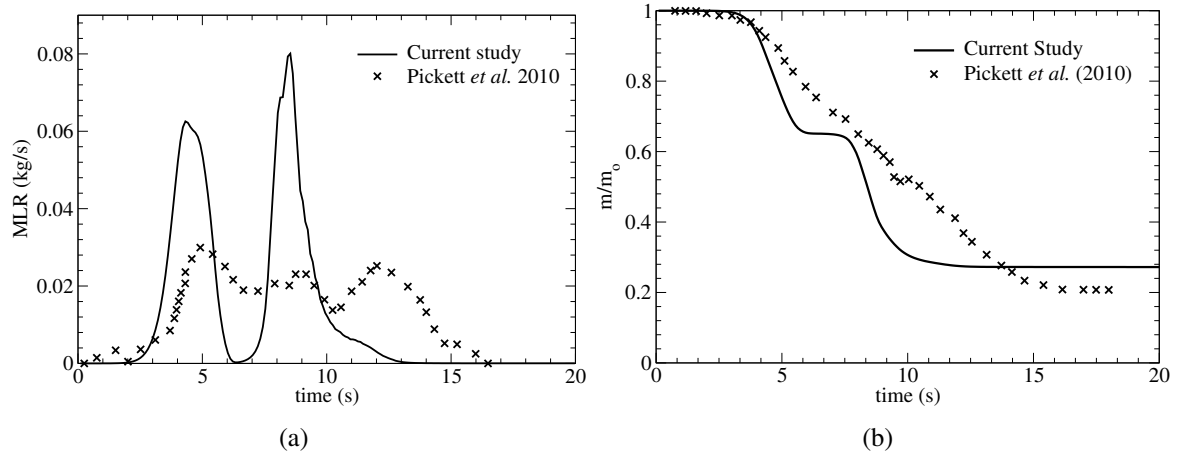
Figure 3: Time histories of (a) mass loss rate, (b) normalised mass (solid line) with experimental results of Pickett *et al.* [12] (symbols) for an initial FMC of 76%.
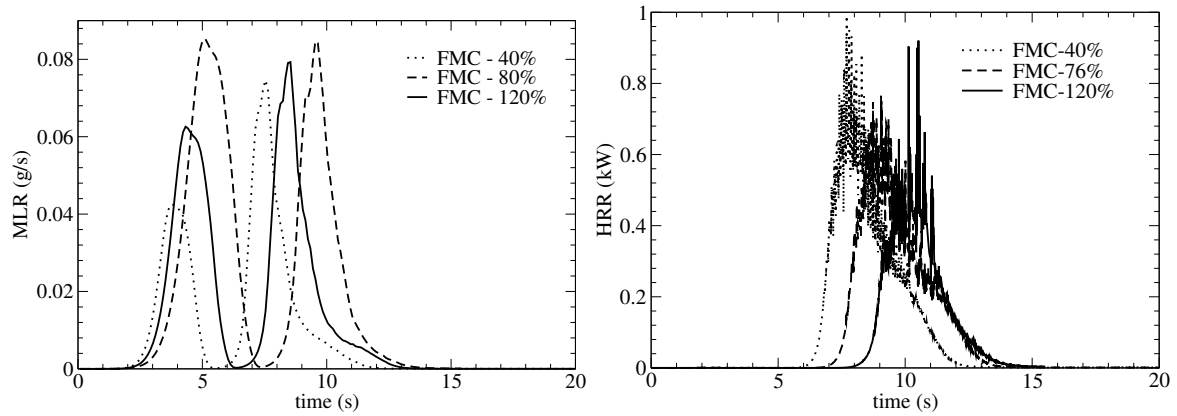

Figure 4: Time histories of (a) mass loss rates, (b) heat release rates for three cases with an initial FMC of 40, 76 and 120%.
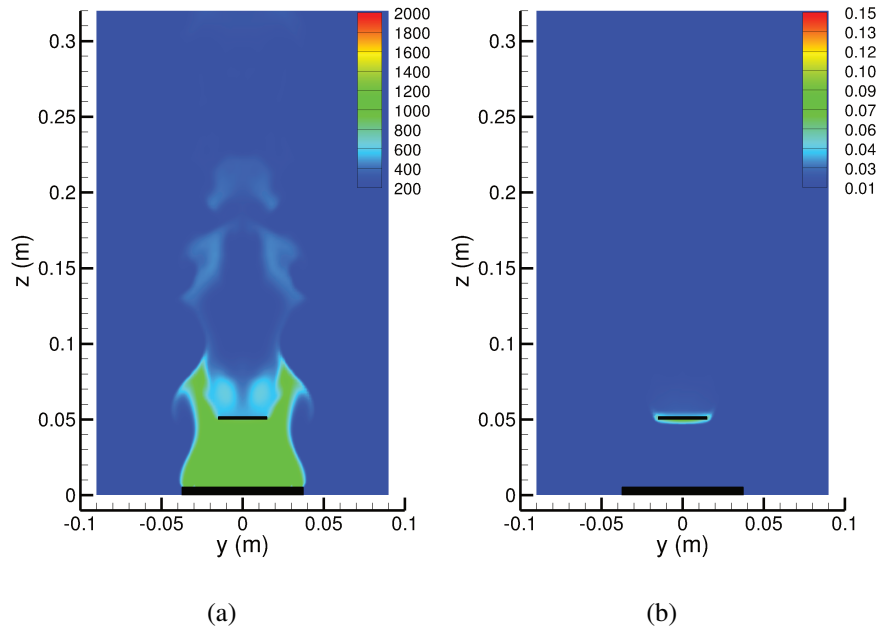
Figure 5: Color contours of (a) temperature, and (b) mass fraction of water vapor in the gas phase at $t =$3 s on an xz-slice located at $y =$0 for a case with an initial FMC of 76%.
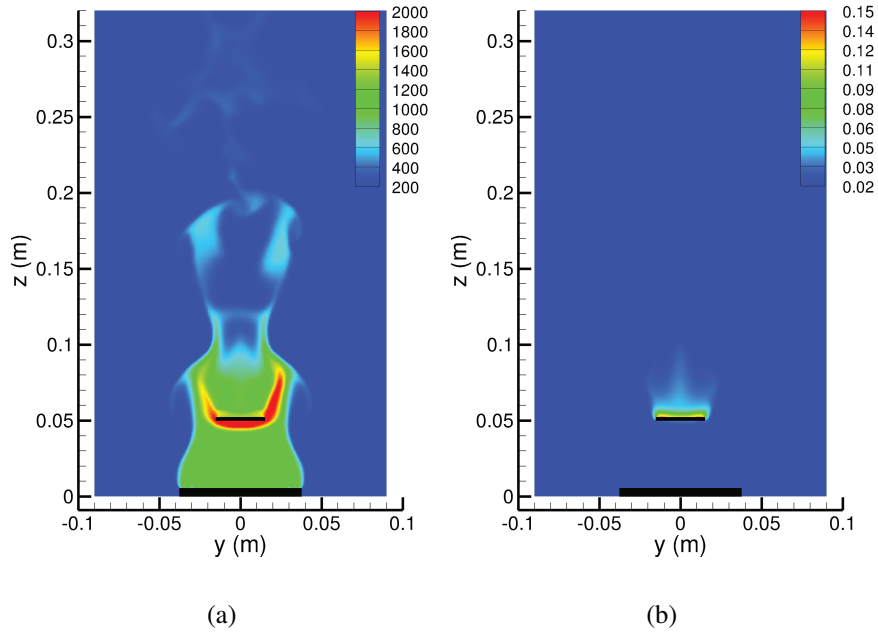

Figure 6: Color contours of (a) temperature, and (b) mass fraction of water vapor in the gas phase at $t =$8 s on an xz-slice located at $y =$0 for a case with an initial FMC of 76%.